Fabrication and photoluminescent characteristics of ZnO/Mg_{0.2}Zn_{0.8}O coaxial nanorod single quantum well structures

Jun Young Bae, Jinkyoung Yoo, and Gyu-Chul Yi^{a)}
National CRI Center for Semiconductor Nanorods, and Department of Materials Science and Engineering,
POSTECH, Pohang, Gyeongbuk 790-784, Korea

(Received 28 July 2006; accepted 11 September 2006; published online 25 October 2006)

The authors report on fabrication and photoluminescent (PL) properties of $ZnO/Mg_{0.2}Zn_{0.8}O$ coaxial nanorod quantum structures with various quantum well and barrier layer thicknesses. Employing catalyst-free metal-organic vapor-phase epitaxy, coaxial nanorod single quantum well structures were fabricated by the alternate heteroepitaxial growth of ZnO and $Mg_{0.2}Zn_{0.8}O$ layers over the entire surfaces of the ZnO nanorods with fine thickness controls of the layers. The quantum confinement effect of carriers in coaxial nanorod quantum structures depends on the $Mg_{0.2}Zn_{0.8}O$ quantum barrier layer thickness as well as the thickness of the ZnO quantum well layer. The temperature-dependent PL characteristics of the coaxial nanorod quantum structures are also discussed. © 2006 American Institute of Physics. [DOI: 10.1063/1.2364463]

One-dimensional semiconductor nanorod heterostructures have great potential for use as functional components for nanometer-scale electronics and optoelectronics. ¹⁻⁴ In particular, heteroepitaxial nanorod quantum structures with well-defined interfaces greatly increase the versatility and power of building blocks used in many nanoscale devices. Two types of nanorod quantum structures are possible, depending on the composition modulation along either the axial or radial direction of the nanorods. Nanorod quantum structures with composition modulation along the radial direction can be formed into coaxial nanorod quantum structures when the overlayers in the quantum structures are covered uniformly and homogeneously over the side walls. For these coaxial nanorod quantum structures, the carriers are confined to the quantum wells, generating one or more welldefined bound states in the wells. Because of the quantum effect, the wavelength of the emitted light can be tuned by changing the thickness of the quantum well, and the characteristics of the light emitting device can also be significantly enhanced. In addition, carriers can be cylindrically localized in the quantum well, resulting in the formation of low dimensional carrier gas. These quantum phenomena are necessary for applications of many sophisticated quantum devices as well as high speed electronic devices.

ZnO is a well known wide band gap semiconductor with a fundamental band gap energy of 3.3 eV at room temperature. As a wide band gap semiconductor, ZnO exhibits heavy effective electron and hole carrier masses of $0.28m_{\rm e}$ and $1.8m_{\rm e}$, much larger than those of narrow band gap semiconductors such as InAs and InP. Since the Bohr radius of a free exciton in ZnO is as small as 1.8 nm, quantum size effects are not observed for homogeneous ZnO nanorods unless the diameter of the ZnO nanorods is comparable to the Bohr radius. Even for ultrafine ZnO nanorods with a diameter of 8 nm, the photoluminescence (PL) blueshift is only $42 \text{ meV}.^5$ However, quantum phenomena can appear for ZnO/ZnMgO nanorod quantum structures with composition modulation along either the axial or radial direction. $^{4.6-8}$

These nanorod quantum structures exhibit a blueshift in the band edge PL peak due to a quantum confinement effect in ZnO well layers between the ZnMgO barrier layers. A6-9 Meanwhile, several studies have reported on coaxial nanorod heterostructures including Ge/Si, Si/CdSe, and GaP/GaN. However, quantum effects in coaxial nanorod quantum structures have rarely been reported, and quantum confinement effect in the coaxial nanorod quantum structures has not thoroughly been studied. Here, we report on comprehensive studies of the fabrication and photoluminescent properties of ZnO/Mg_{0.2}Zn_{0.8}O coaxial nanorod quantum structures with a single quantum well layer.

 $ZnO/Mg_{0.2}Zn_{0.8}O$ coaxial nanorod quantum structures were fabricated on Si substrates by catalyst-free metalorganic chemical vapor deposition (MOCVD).^{5,12} Prior to the growth of the nanorod quantum structures, core ZnO nanorods were grown on Si substrates using diethylzinc and oxygen as reactants, with argon as the carrier gas. No metal catalyst was used for the ZnO nanorod growth. Depending on the growth conditions, the mean diameters of the ZnO nanorods could be controlled in the range of 8-70 nm. The subsequent deposition of a Mg_{0.2}Zn_{0.8}O shell layer were performed in situ by the addition of biscyclopentadienyl-Mg (cp₂Mg) as the Mg precursor in the same chamber, resulting in Mg_{0.2}Zn_{0.8}O layer coating on the entire surfaces of the ZnO nanorod surfaces. The average concentration of Mg in the Mg_{0.2}Zn_{0.8}O layers was about 20 at %, as determined by energy dispersive x-ray spectroscopy in a transmission electron microscopy (TEM) chamber. The ZnO/Mg_{0.2}Zn_{0.8}O coaxial nanorod quantum structures, schematically depicted in Fig. 1(a), were prepared by the repeated alternate deposition of ZnO quantum well (QW) and Mg_{0.2}Zn_{0.8}O quantum barrier (QB) layers. For the fabrication of such sophisticated coaxial nanorod quantum structures, the ZnO QW and Mg_{0.2}Zn_{0.8}O QB layer thicknesses were precisely controlled on an angstrom scale using a computer-controlled gas valve system in MOCVD. The nanorod diameters were determined by transmission electron microscopy. The ZnO well and Mg_{0.2}Zn_{0.8}O barrier layer thicknesses increased in proportion to growth time with typical growth rates of 0.25 and 0.33 Å/s, respectively.

a) Author to whom correspondence should be addressed; electronic mail: gcyi@postech.ac.kr

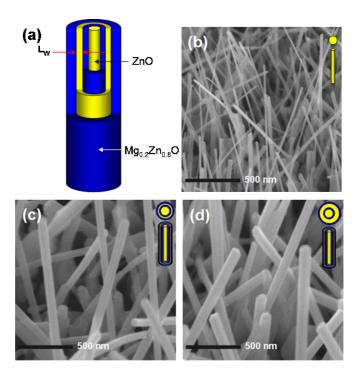


FIG. 1. (Color online) (a) Schematic and [(b)-(d)] SEM images of ZnO/Mg_{0.2}Zn_{0.8}O coaxial nanorod quantum structures with various single quantum well shell layer thicknesses of 8-45 Å.

The quantum confinement effect of ZnO/Mg_{0.2}Zn_{0.8}O coaxial nanorod quantum structures were investigated by measuring PL spectra of the nanorod quantum structures at various temperatures in the range of 10-300 K. The PL measurements were performed using the 325 nm line of a He-Cd laser as an excitation source. Details in the PL measurement are described elsewhere. 13

Figures 1(b)-1(d) show field-emission scanning electron microscopy (FE-SEM) images of bare ZnO nanorods and ZnO/Mg_{0.2}Zn_{0.8}O coaxial nanorod single quantum well structures with various well layer thicknesses. As shown in Fig. 1(b), bare ZnO nanorods with a mean diameter of 26 nm and a length of 2.5 μ m were grown at 800 °C for 2 h. The continuous growth of the ZnO QW and Mg_{0.2}Zn_{0.8}O QB layers leads to an increase in core/multishell nanorod diameter. In comparison to bare ZnO nanorods, no significant change in the morphology was found except that the nanorod diameters increased with the coating time of the ZnO well and the Mg_{0.2}Zn_{0.8}O barrier layers. From FE-SEM and TEM measurements, typical diameters of ZnO/Mg_{0.2}Zn_{0.8}O coaxial nanorod single quantum well structures with ZnO well layers grown for 30 and 180 s, and a Mg_{0.2}Zn_{0.8}O barrier layer grown for 3 min, were estimated to be 51 and 58 nm, respectively, a significant increase from the 26 nm average diameter of ZnO core nanorods. Although there is no way to accurately determine the growth rate of each layer in the nanorod heterostructures due to the large variation in nanorod diameters on the same substrate, averaging the diameters of the individual core/multishell nanorods from microscopic images suggests that the average growth rates of the ZnO (QW) and Mg_{0.2}Zn_{0.8}O (QB) shells were roughly 0.25 and 0.33 Å/s, respectively.

A quantum confinement effect along the radial direction in ZnO/Mg_{0.2}Zn_{0.8}O coaxial nanorod single quantum well structures was observed in low temperature PL measurements. Figure 2 shows 10 K PL spectra of ZnO/Mg_{0.2}Zn_{0.8}O Downloaded 27 Oct 2006 to 141.223.168.250. Redistribution subject to AIP license or copyright, see http://apl.aip.org/apl/copyright.jsp

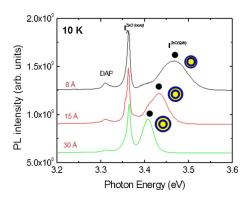


FIG. 2. (Color online) Low temperature PL spectra of ZnO/Mg_{0.2}Zn_{0.8}O coaxial nanorod quantum structures with various well layer thicknesses (L_w) of 8, 15, and 30 Å.

coaxial nanorod single quantum well structures with different well layer widths of 8, 15, and 30 Å. In addition to the PL peak at 3.364 eV corresponding to excitonic emissions from ZnO core nanorods ($I_2^{\rm ZnO~(core)}$), the PL spectra of the ZnO/Mg_{0.2}Zn_{0.8}O coaxial nanorod single quantum well structures exhibited two dominant PL peaks at 3.364 eV, corresponding to excitonic emissions from the ZnO core nanorods $(I_2^{\text{ZnO (core)}})$; a new PL peak denoted as $I^{\text{ZnO (QW)}}$ was observed at 3.467, 3.433, and 3.409 eV, depending on the thickness of the ZnO (QW) shell thickness. For a ZnO (QW) shell thickness of 30 Å, the I^{ZnO} (QW) peak energy was blueshifted by 45 meV and the I^{ZnO} (QW) peak energy in Fig. 2 was blueshifted by up to 3.467 eV with a difference of 103 meV compared to the $I_2^{\text{ZnO (core)}}$ peak energy as the ZnO (QW) shell width is gradually decreased from 30 to 8 Å. Such a blueshift in the PL emission peak can be rationalized by the fact that quantized sublevel states are created due to quantum size effects in the core/multishell nanorod heterostructures and the quantized energy levels increase with a decrease in the embedded ZnO (QW) shell layer width.

PL spectra of the coaxial nanorod quantum structures with various QB layer thicknesses were measured to investigate the effect of QB layer thickness on the quantum confinement of the carriers. Figure 3 shows 10 K PL spectra of the coaxial nanorod quantum structures with a ZnO core diameter of 50 nm, a ZnO QW layer thickness of 1.5 nm, and various QB layer thicknesses of 1.5, 3, 6, and 18 nm. For a QB layer thickness of 18 nm, a strong PL peak was observed at 3.427 eV, resulting from the quantum confinement effect

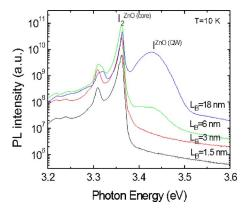


FIG. 3. (Color online) Low temperature PL spectra of ZnO/Mg_{0.2}Zn_{0.8}O coaxial nanorod quantum structures with various barrier layer thicknesses (L_R) of 1.5, 3, 6, and 18 nm.

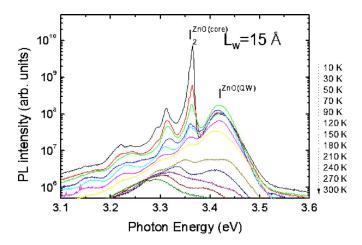


FIG. 4. (Color online) Temperature-dependent PL spectra o $ZnO/Mg_{0.2}Zn_{0.8}O$ coaxial nanorod quantum structures with L_W of 15 Å.

in a single ZnO quantum well layer. The intensity of the PL peak decreased significantly with the decrease in QB layer thickness to 6 nm, and then totally disappeared for QB layer thicknesses of 1.5 and 3 nm. This suggests that a QB layer thickness of 6 nm is too thin to confine the carriers or that the QB layers are not uniformly covered with holes present resulting in carrier leakage.

Meanwhile, it may be argued that the blueshift in the PL peak results from the intermixing of ZnO and Mg_{0.2}Zn_{0.8}O, in which the previous reactants are not purged for a sufficiently long time. In this case the PL blueshift originates from the intermixing, resulting in the Mg mole fraction in the alloy becoming higher with increasing Mg_{0.2}Zn_{0.8}O shell layer thickness (or growth time), and in a larger blueshift in the PL peak. However, as shown in Fig. 3, the *I*^{ZnO} (QW) peak position did not depend on the QB layer thickness of the coaxial nanorod quantum structures. This result was also clearly confirmed from PL spectra for thicker QB layer thicknesses of 12 and 78 nm, indicating that the PL blueshift in the coaxial nanorod quantum structures results from a quantum confinement effect rather than the composition intermixing.

Further optical properties of ZnO/Mg_{0.2}Zn_{0.8}O coaxial nanorod quantum structures were investigated by measuring their temperature-dependent PL spectra in the range of 10–300 K. Figure 4 shows the temperature-dependent PL spectra of ZnO/Mg_{0.2}Zn_{0.8}O coaxial nanorod quantum structures with a L_W of 15 Å. The energy positions of donor bound exciton peak, $I_2^{\rm ZnO~(core)}$ and $I^{\rm ZnO~(QW)}$, decreased with band gap energy shrinkage, and the PL peak intensities decreased with increasing temperature. However, the thermal quenching behavior of $I^{\rm ZnO~(CW)}$ was different from that of $I^{\rm ZnO~(core)}$: the $I^{\rm ZnO~(core)}$ peak intensity decreased drastically

and disappeared at temperatures above 120 K, whereas the $I^{\rm ZnO~(QW)}$ peak quenched slowly and survived at 300 K. The low thermal quenching of the $I^{\rm ZnO~(QW)}$ peak presumably results from the quantum confinement effect of carriers in the quantum well and also implies that the structural quality of coaxial nanorod quantum structures is high with clean ${\rm ZnO/Mg_{0.2}Zn_{0.8}O}$ interfaces because PL quenching is also related to interfacial defects.

Our controlled growth of ZnO/Mg_{0.2}Zn_{0.8}O coaxial nanorod single quantum well structures opens up significant opportunities for the fabrication of oxide-based quantum device structures with radial composition modulation. The oxide-based coaxial nanorod quantum structures were produced by the alternative heteroepitaxial growth of ZnO and Mg_{0.2}Zn_{0.8}O layers on ZnO nanorod surfaces. The quantum confinement in the ZnO/Mg_{0.2}Zn_{0.8}O coaxial nanorod quantum well structures was dependent on the Mg_{0.2}Zn_{0.8}O barrier layer thickness as well as the ZnO well layer thickness. These quantum building blocks create well-defined potential profiles along the radial direction in nanorod heterostructures, which would be useful for high electron mobility nanotransistors and light-emitting devices.

This work was financially supported under the National Creative Research Initiative Project by the KOSEF.

¹L. J. Lauhon, M. S. Gudiksen, D. Wang, and C. M. Lieber, Nature (London) **420**, 57 (2002).

²J. Goldberger, R. He, Y. Zhang, S. Lee, H. Yan, H.-J. Choi, and P. Yang, Nature (London) **422**, 599 (2003).

³M. T. Björk, B. J. Ohlsson, T. Sass, A. I. Persson, C. Thelander, M. H. Magnusson, K. Deppert, L. R. Wallenberg, and L. Samuelson, Appl. Phys. Lett. 80, 1058 (2002).

⁴W. I. Park, G.-C. Yi, M. Kim, and S. J. Pennycook, Adv. Mater. (Weinheim, Ger.) **15**, 526 (2003).

W. I. Park, J. Yoo, and G.-C. Yi, J. Korean Phys. Soc. 46, L0167 (2005).
 W. I. Park, S. J. An, J. L. Yang, G.-C. Yi, S. Hong, T. Joo, and M. Kim, J. Phys. Chem. B 108, 15457 (2004).

⁷W. I. Park, J. Yoo, D.-W. Kim, G.-C. Yi, and M. Kim, J. Phys. Chem. B **110**, 1516 (2006).

⁸E.-S. Jang, J. Y. Bae, J. Yoo, W. I. Park, D.-W. Kim, G.-C. Yi, T. Yatsui, and M. Ohtsu, Appl. Phys. Lett. **88**, 023102 (2006).

⁹S. S. Kim, H. J. Lim, H. Cheong, W. I. Park, and G.-C. Yi, J. Korean Phys. Soc. **46**, S214 (2005).

¹⁰Q. Li and C. Wang, J. Am. Chem. Soc. **125**, 9892 (2003).

¹¹H.-M. Lin, Y.-L. Chen, J. Yang, Y.-C. Liu, K.-M. Yin, J.-J. Kai, F.-R. Chen, L.-C. Chen, Y.-F. Chen, and C.-C. Chen, Nano Lett. 3, 537 (2003).

¹²W. I. Park, D. H. Kim, S. W. Jung, and G.-C. Yi, Appl. Phys. Lett. **80**, 4232 (2002).

¹³S. W. Jung, W. I. Park, H.-D. Cheong, G.-C. Yi, H. M. Jang, S. Hong, and T. Joo, Appl. Phys. Lett. **80**, 1924 (2002).

¹⁴W. I. Park, G.-C. Yi, and H. M. Jang, Appl. Phys. Lett. **79**, 2022 (2001).

¹⁵A. Ohtomo, M. Kawasaki, T. Koida, K. Masubuchi, H. Koinuma, Y. Sakurai, Y. Yoshida, T. Yasuda, and Y. Segawa, Appl. Phys. Lett. **72**, 2466 (1998).